

# Online Condition Monitoring of Battery Systems With a Nonlinear Estimator

Günyaz Ablay, *Member, IEEE*

**Abstract**—The performance of batteries as uninterruptable power sources in any industry cannot be taken for granted. The failures in battery systems of safety-related electric systems can lead to performance deterioration, costly replacement, and, more importantly, serious hazards. The possible failures in battery systems are currently determined through periodic maintenance activities. However, it is desirable to be able to detect the underlying degradation and to predict the level of unsatisfactory performance by an online real-time monitoring system to prevent unexpected failures through early fault diagnosis. Such an online fault diagnosis method can also contribute to better maintenance and optimal battery replacement programs. A robust nonlinear estimator-based online condition monitoring method is proposed to determine the state of health of the battery systems online in industry. Real-world experimental data of a modern battery system are used to assess the efficiency of the proposed approach in the existence of parameter uncertainties.

**Index Terms**—Battery management, battery modeling, condition monitoring, fault diagnosis.

## I. INTRODUCTION

THE increasing needs for high energy, power, life-cycle, FUEL economy, wide-range operating temperature, and environmentally acceptable batteries in electric and hybrid electric systems are the driving forces for rapid growth of battery technologies. While there are many battery types, some batteries are more preferable to others in certain industries. For example, Ni-MH batteries are dominant battery technology for hybrid electric vehicle applications by having the best overall performance in the wide-range requirements set by automobile companies [1]. The nuclear plants benefit from lead-acid batteries for their wide range of electrical systems as battery-backed supplies (UPSs) to ensure continuity of function during outages or interruptions [2], [3]. Fig. 1 shows a general working principle of the battery systems in various industries. The dc load is powered from battery chargers (rectifiers) during normal operation, and it is automatically powered from station batteries in case of loss of normal power to the battery chargers.

Reliability of the battery system is significant for any industry due to the safety-related usage aim of the batteries. There

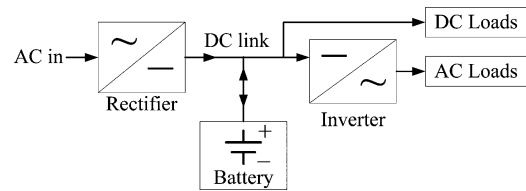


Fig. 1. General working principle of battery systems.

are many factors that cause failures in battery systems, including design errors, battery component failures, overloading of dc busses, flaking of cell plates, and aging-related failures [3], [4]. For these reasons, monitoring and maintenance activities are necessary for battery systems. Many industries (e.g., nuclear power plants) perform periodic maintenance (monthly, quarterly, and yearly) and battery parameter testing (capacity and internal ohmic tests) for battery systems within the maintenance program. The functionality and reliability of batteries can be enhanced with online fault diagnosis and health monitoring. The diagnostic algorithm can monitor the battery system for any possible faults and malfunctions. A battery monitoring system is specifically necessary for sealed batteries, e.g., valve regulated lead-acid and lithium-ion batteries, since it is not possible to directly measure their internal parameters, i.e., internal cell resistances. It helps in detecting deviations of the battery performance from its normal behavior and also isolates the possible causes for the faults. In practice, output signals (measurements) of the system under consideration are often directly evaluated and compared with a given threshold [5]. However, such an approach is insufficient in critical processes due to capability to react only after a relatively large change in the measured variable [6], [7]. If the system is modeled, and the difference between the measurement and its estimation (residual) is obtained, then it is theoretically possible to detect every fault with residual generation [8], [9]. The measurements of rechargeable batteries are current and voltage at the poles of the batteries and the battery temperature, which are enough to model the battery system for fault diagnosis and health monitoring in order to prevent serious damage and failures and to have better maintenance activities. In the literature, most of the fault diagnosis and health monitoring studies are provided for lithium-ion batteries due to their usage in wide-range applications. The approaches include extended Kalman filter, autoregressive moving average model, and fuzzy logic, which are summarized in [10], model-based state-of-charge (SOC) estimation [11], model-based fault diagnosis algorithm [12], and parabolic regression algorithm [13]. However, the robustness and efficiency of the above estimation approaches are questionable due to parameter uncertainties, simplifications, and linearization in the models.

Manuscript received July 5, 2013; revised September 23, 2013 and October 21, 2013; accepted November 14, 2013. Date of publication December 3, 2013; date of current version February 14, 2014. Paper no. TEC-00379-2013.

The author is with the Department of Electrical-Electronics Engineering, Abdullah Gul University, 38039 Kayseri, Turkey (e-mail: gunyaz.ablay@agu.edu.tr).

Color versions of one or more of the figures in this paper are available online at <http://ieeexplore.ieee.org>.

Digital Object Identifier 10.1109/TEC.2013.2291812

In this study, a robust nonlinear estimator-based online condition monitoring methodology is proposed for robust fault diagnosis in battery systems in the presence of parameter uncertainties that make the previous studies questionable. In reality, the periodic maintenance activities are the only way to determine health of a battery in industries, e.g., nuclear power plants. With the usage of the proposed online condition monitoring approach, unexpected failures can be prevented by early fault detection, and optimization in the replacement programs and better maintenance activities can be obtained efficiently.

The organization of the paper is as follows. Section II describes the characterization and modeling of battery systems. Section III describes the design, synthesis, and analysis of online condition monitoring strategy. The assessments and conclusions are given in Sections IV and V, respectively.

## II. BATTERY SYSTEMS

There have been significant developments in battery technologies that offer excellent advantages, including flexible cell sizes from 30 mAh to 250 Ah, safe operation at high voltage (+320 V), high volumetric energy and power, maintenance-free designs, excellent thermal properties, environmentally acceptable and recyclable materials, and simple and inexpensive charging and electronic control circuits [1], [14]. The lithium-ion and especially nickel–metal hydride (Ni-MH) batteries are the current batteries that can provide the above advantages. However, the common use of these new rechargeable battery systems in UPSs and industry requires further studies and new technical standards.

The electrochemistry of rechargeable batteries is based on charge-discharge mechanism between positive and negative electrodes. The electricity generation processes in a battery cell are chemical reactions that either consume or release electrons as the electrode reaction proceeds to completion. Such reaction, depending on battery electrode and electrolyte materials and mechanisms that affect battery terminal voltage, is similar to all types of batteries. Battery terminal voltage changes with the electrolyte concentration and there are resistive drops in electrodes with current flow [15].

To extend the life of a battery system, charge and thermal managements play important roles and any problem related to overcharge, overdischarge, or control system must be diagnosed with an online condition monitoring system. For developments of online real-time battery monitoring systems, the large-scale storage batteries have been commonly modeled in three ways: equivalent circuit battery models [16]–[19], electrochemical battery models [20]–[23], and correlation-based models [24]. Since electrochemical and experimental models are not well suited to demonstrate battery dynamics accurately [25], the equivalent circuit battery model that is based on current-voltage relations of the batteries is considered in this study.

The battery system consists of two main subsystems: battery package and temperature controller. Considering battery (load) current as an input, and battery voltage and temperature as outputs, the battery model consists of three submodels: electrical,

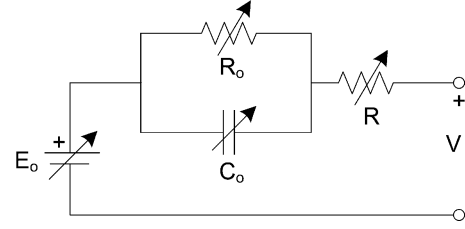


Fig. 2. Battery Thevenin equivalent model.

TABLE I  
EXPERIMENTAL BATTERY PARAMETERS

	Discharge ( $I > 0$ )		Charge ( $I < 0$ )	
$R_o$ (in Ohms)	$1.6 \times 10^{-3} - 2.5 \times 10^{-5} * S * T$		$(8.3 - 2.2 * T - 3.6 * S) \times 10^{-3}$	
$C_o$ (in Farads)	1500		1500	
$R$ (in Ohms)	$4.3 \times 10^{-3} - 4.4 \times 10^{-5} * T$		$4.3 \times 10^{-3} - 4.4 \times 10^{-5} * T$	
$E_o$ (in Volts)	$1.19 + 0.09 * S + 0.001 * T$		$1.19 + 0.09 * S + 0.001 * T$	
Other parameters				
$mc$	50 J/°C	$hA$	0.07 J/°C	$T_\infty$ 20 °C
$C_n$	10 Ah	$N$	250 cells	$f_{s0}$ 0

thermal, and SOC models. Each of these submodels is described below.

### A. Electrical Model

The voltage (capacity) in the battery cells is represented by a voltage source, the electrochemical delay of the battery due to shifting ion concentrations and plate current densities is described by a capacitor–resistor model, and the internal resistance of the battery due to electrolyte diffusion is modeled by a resistor [26], [27]. The most commonly used battery models are ideal model, linear model, and Thevenin equivalent model [16], [28], [29]. The Thevenin equivalent model with varying parameters due to temperature and SOC variations represents batteries with higher accuracy, as experimentally shown in many studies [30], and thus, it is considered in this study. This model is made of electrical values of the open-circuit voltage ( $E_o$ ), internal resistance ( $R$ ), capacitance ( $C_o$ ), and the over-voltage resistance ( $R_o$ ) [16]. The Thevenin equivalent model of a battery is depicted in Fig. 2.

From Fig. 2, the dynamic electric equations of the circuit can be obtained by applying Kirchhoff’s rules as

$$\begin{cases} \frac{dV_c}{dt} = -\frac{1}{R_o C_o} V_c + \frac{1}{C_o} I \\ V = E_o - RI - V_c \end{cases} \quad (1)$$

where  $I$  (in Amperes) is the current at the input,  $V_c$  (in Volts) is the capacitance voltage and  $V$  (in Volts) is the output voltage. All the parameters of (1) are functions of battery temperature ( $T$  in °C) and SOC (denoted by  $S$ ), and can be different in charge and discharge phases. The battery parameters are determined using experimental battery charge and discharge data for a Ni-MH battery system, and given in Table I. The meanings of the parameters described by “other parameters” in Table I are explained in Section II-C. The data used in this study were acquired as part of the activities of the Center for Automotive Research at the Ohio State University. A general structure of the battery test system is illustrated in Fig. 3. The test system

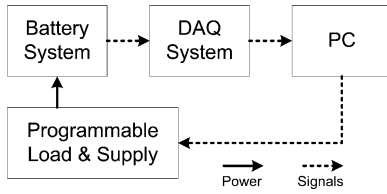


Fig. 3. Battery test system.

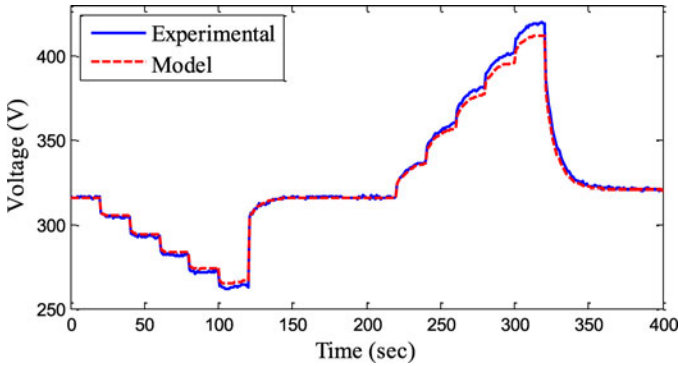


Fig. 4. Battery electrical model validation using voltage measurements at room temperature.

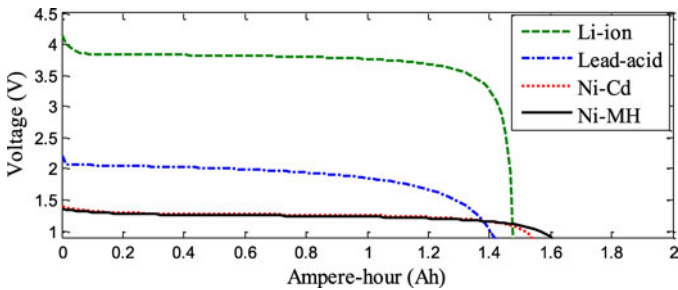


Fig. 5. Nominal current discharge characteristics for different types of batteries.

is appropriate for modeling any battery systems. With the use of this battery test system, the accuracy of the battery electrical model is tested and showed in Fig. 4. As seen from Fig. 4, the battery model has a good level of accuracy.

To represent a particular battery type, the parameters of the electrical model can be changed depending on its discharge characteristics as illustrated in Fig. 5. It can be seen from the figure that the exponential voltage drop sections of the batteries can have more or less wide areas depending on the battery type. The parameters gathered from the discharge characteristics are usually assumed to be the same for charging when the electrical model parameters are determined.

### B. SOC Model

SOC provides information about remaining useful energy and the remaining usable time of the battery. Many systems are sensitive to overcharge and too high or too low SOC can result in irreversible damage in the battery. It can be difficult to measure the SOC in the battery systems depending on the type and application of the battery. There have been a num-

ber of different modeling approaches in the literature including discharge test, ampere hour counting, linear model, impedance spectroscopy, internal resistance, Kalman filter, and open-circuit voltage model [10], [31]–[33]. One of the most acceptable SOC calculation methods is the ampere hour counting (current integration) method [10], [31] defined by

$$S = S_0 - \frac{1}{C_n} \int_0^t I(t) dt \quad (2)$$

where  $I$  (in Amperes) is the battery (load) current,  $C_n$  (in Ampere-hours) is the nominal capacity, and the initial SOC is given by  $S_0$ . This approach requires dynamic measurement of the battery current. It is applicable to all battery systems, easy to calculate and accurate with good current measurements.

Practically, the operating range of batteries with respect to SOC is confined with specific numbers. For example, a Ni-MH battery has an operating range around 40–80% with respect to SOC. Hence, this method implies that the charging operation is controlled.

### C. Thermal Model

In many systems, it is critical to achieve performance and extended life of batteries through thermal management. Rechargeable batteries are designed to work in room temperature (25 °C), but a battery cannot be held at a certain temperature due to daily and seasonal temperature changes. It is well known that low temperatures slow up the chemical reactions in any battery, resulting in reduced performance; however, from the other extreme high temperatures destroy batteries. According to the Arrhenius equation [34], for every 10 °C increase in battery temperature, battery life is halved due to faster positive grid corrosion. Suitable modeling for predicting thermal behavior of battery systems in applications can help to improve battery design and development process. Therefore, thermal models for batteries have been developed based on thermal energy balance of batteries, and they are coupled with electrochemical or electric models [21], [22]. Based on the electric model and thermal energy balance of a battery, a simple thermal model can be built as

$$\frac{dT}{dt} = \frac{R + R_o}{mc} I^2 - \frac{hA}{mc} (T - T_\infty) \quad (3)$$

where  $mc$  (in  $J/^\circ C$ ) is the effective heat capacity per cell,  $hA$  (in  $J/^\circ C$ ) is the effective heat transfer per cell, and  $T_\infty$  (in  $^\circ C$ ) is the bulk temperature. The effective heat transfer capacity per cell is given in terms of temperature controller (fan) settings by

$$hA = h_0 A_0 (1 + 0.5 f_s) \quad (4)$$

where  $h_0 A_0$  (in  $J/^\circ C$ ) is given in Table I for natural convection, and the controller setting  $f_s$  depends on the temperature. In this study, the following temperature controller settings will be used:

$$\begin{cases} f_s = 0 \text{ off mode,} & f_s = 1 \text{ if } T \geq 30^\circ C \\ f_s = 2 \text{ if } T \geq 35^\circ C & f_s = 3 \text{ if } T \geq 40^\circ C. \end{cases} \quad (5)$$

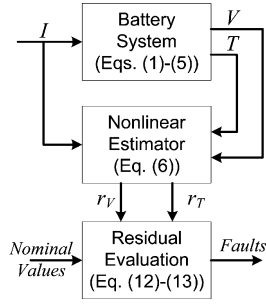


Fig. 6. Fault diagnosis scheme for the battery system.

### III. ONLINE CONDITION MONITORING IN BATTERY SYSTEMS

The model of battery systems is complicated due to the feedback loop and the state-dependent and time-varying parameters. The equivalent electrical model parameters of batteries are functions of temperature and SOC, which make fault detection difficult. Moreover, the temperature feedback controller can mask the temperature sensor faults so that the detection problem can pose some additional challenges. A model-based online condition monitoring scheme for the battery systems is illustrated in Fig. 6. The residual generator is composed of a nonlinear estimator, and the residual evaluation subsystem is used to provide fault information by comparing the residuals with their nominal values. The residual generator and evaluation algorithms are designed below to detect and isolate possible system faults online.

#### A. Robust Nonlinear Estimator for Residual Generation

A robust nonlinear estimator-based approach is considered to generate residuals in this study. The main advantages of this approach are robustness and high precision state estimation in the presence of parameter variations. These features of the nonlinear estimator can enhance detection of internal battery problems through detection of internal cell resistance variations. Based on the system model given in (1)–(5), a nonlinear estimator can be designed as

$$\begin{cases} \frac{d\hat{T}}{dt} = \frac{\hat{R} + \hat{R}_o}{mc} I^2 - \frac{\hat{h}A}{mc} (\hat{T} - T_\infty) + \delta_1 \text{sign}(T - \hat{T}) \\ \frac{d\hat{V}_c}{dt} = -\frac{1}{\hat{R}_o C_o} \hat{V}_c + \frac{1}{C_o} I \\ \hat{V} = \hat{E}_o - \hat{R}I - \hat{V}_c \\ \hat{h}A = h_0 A_0 (1 + 0.5 \hat{f}_s) \end{cases} \quad (6)$$

where  $(\hat{T}, \hat{V}_c, \hat{V})$  are the estimates of  $(T, V_c, V)$ , the observer gain  $\delta_1$  is a constant to be selected, and the  $\text{sign}(\cdot)$  function is the unit vector defined by

$$\text{sign}(e) = e/|e| \quad (7)$$

where  $e_T$  is the error state defined by  $e_T = T - \hat{T}$ . The nonlinear estimator gain  $\delta_1$  must be selected large enough to bring the estimation errors to zero as explained in the following section.

#### B. Dynamical Analysis of the Residual Generator

By considering dynamic equations (1) and (3), the state space form of the battery model can be written as

$$\begin{bmatrix} dV_c/dt \\ dT/dt \end{bmatrix} = \begin{bmatrix} -k_1 & 0 \\ 0 & -k_2 \end{bmatrix} \begin{bmatrix} V_c \\ T \end{bmatrix} + \begin{bmatrix} b_1 \\ b_2 I \end{bmatrix} I + \begin{bmatrix} 0 \\ k_2 \end{bmatrix} T_\infty \quad (8)$$

where  $k_1 = 1/R_o C_o$ ,  $k_2 = hA/mc$ ,  $b_1 = 1/C_o$ , and  $b_2 = (R + R_o)/mc$ . Since  $I$  and  $T_\infty$  are bounded, i.e.,  $\sup |I(t)| < I_m$  for  $I_m < \infty$  and  $\sup |T_\infty(t)| < T_m$  for  $T_m < \infty$ , and it is evident from the system matrix that the battery system has two distinct and negative eigenvalues,  $\lambda_{V_c} = -k_1$  and  $\lambda_T = -k_2$ . Hence, battery systems have stable dynamics. Here,  $V_c(t)$  has much faster stable dynamics than  $T(t)$  since  $|\lambda_{V_c}| \gg |\lambda_T|$ , implying that the slow state variable  $T(t)$  determines the dynamic behavior of the battery system under bounded input values. It is clear from (8) that the dynamics of  $V_c$  and  $T$  are almost completely independent of each other (uncoupled). Temperature  $T$  is a directly measurable state, but capacitance voltage  $V_c$  is an indirectly measurable state through battery voltage  $V$  as given in (1). For these reasons, the error dynamics of the estimator can be analyzed separately.

To analyze the stability of the nonlinear estimator (6), first we can consider the temperature estimation error  $e_T = T - \hat{T}$ . The dynamic of the temperature estimation error is

$$\dot{e}_T = -k_2 e_T + (b_2 - \hat{b}_2) I^2 - \delta_1 \text{sign}(e_T). \quad (9)$$

A candidate Lyapunov function [35], [36] can be selected as  $W = e_T^2/2$ ; then, its time derivative is

$$\begin{aligned} e_T \dot{e}_T &= e_T ((b_2 - \hat{b}_2) I^2 - \delta_1 \text{sign}(e_T)) - k_2 e_T^2 \\ &\leq (|(b_2 - \hat{b}_2) I^2| - \delta_1) |e_T| - k_2 e_T^2. \end{aligned} \quad (10)$$

Here, the observer gain  $\delta_1$  is selected large enough to satisfy  $\delta_1 > |(b_2 - \hat{b}_2) I^2|$ . Hence, the derivative of the Lyapunov function turns out to be negative definite,  $e_T \dot{e}_T < 0$ , which indicates error convergence to zero.

Finally, the dynamic of capacitance voltage estimation error  $e_{V_c} = V_c - \hat{V}_c$  can be written as

$$\begin{aligned} \dot{e}_{V_c} &= -k_1 V_c + b_1 I + k_1 \hat{V}_c - b_1 I \\ &= -k_1 e_{V_c}. \end{aligned} \quad (11)$$

It is clear from (11) that  $e_{V_c}$  is going to approach to zero with increasing time since  $k_1 > 0$ . As a result, the estimation errors on the temperature and capacitance voltage decay to zero, i.e.  $e_T \rightarrow 0$ ,  $e_{V_c} \rightarrow 0$ , with some time by choosing the observer gain  $\delta_1$  sufficiently large.

### IV. RESIDUAL EVALUATION

The battery system has three measurements: voltage, temperature as outputs, and a load current input. By using these measurements, it is possible to detect and isolate single faults in temperature and voltage sensors, and internal resistance deviations. In addition, a failure in the temperature controller can be detected.

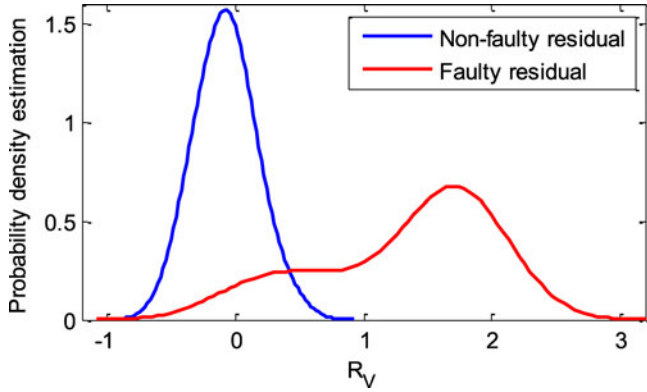


Fig. 7. Probability density estimation for voltage residual (normalized).

The residuals can be acquired with the usage of estimation error states:

$$\begin{cases} r_T \equiv e_T = T - \hat{T} \\ r_V \equiv e_V = V - \hat{V} \end{cases} \quad (12)$$

where  $r_T$  and  $r_V$  are residuals for temperature and voltage measurements, respectively.

The generated residuals can be evaluated based on some threshold selections. There will always be a tradeoff between the avoidance of false alarms and the detection of small faults in the existence of noise and modeling errors. Practically, a fault can be detected only if it causes the residual evaluation function to surpass a threshold [8]

$$|r_i(t)| \geq R_i \quad (13)$$

where  $r_i(t)$  is the function of the  $i$ th residual and  $R_i$  is the selected threshold for  $i$ th residual function.

A systematic threshold selection may be based on the statistical evaluation of the residuals under the absence of the fault since residuals can be degraded by the measurement noise or disturbance. The thresholds for each residual can be calculated from the mean and standard deviation of the corresponding residuals under nonfaulty cases. For example, probability density estimations of the voltage residual under nonfaulty and faulty cases are illustrated in Fig. 7, which shows different mean and standard deviation values for nonfaulty and faulty cases. An optimal threshold value can be the intersection of the probability density functions of nonfaulty and faulty residual signals (see Fig. 7). However, in such a case, the overlapped regions result in either false alarms or missed detections. Therefore, more conservative threshold values must be selected to avoid false alarms. To avoid false alarms, thresholds for residuals  $r_V$  and  $r_T$  can be selected as  $R_V = \mu_V + 4\sigma_V$  and  $R_T = \mu_T + 4\sigma_T$ , similar to the Shewhart control chart [37], where  $\mu_T$  and  $\mu_V$  are the means, and  $\sigma_T$  and  $\sigma_V$  are the standard deviations of related residuals under fault-free cases.

A residual evaluation chart is given in Table II, which shows that single faults can be detected and isolated. The temperature sensor fault and unexpected internal resistance change may not be isolated with the given logic because both affect the same residuals.

TABLE II  
FAULT DIAGNOSIS CHART

Residuals \ Faults	Residual 1 $r_V = V - \hat{V}$	Residual 2 $r_T = T - \hat{T}$
Controller Failure	0	1
Voltage Sensor	1	0
Temperature Sensor	1	1
Resistance Change	1	1

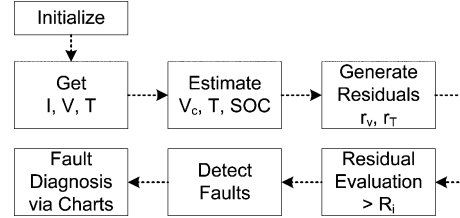


Fig. 8. Flow diagram of the proposed fault diagnosis approach.

A flow diagram of the proposed fault diagnosis approach is illustrated in Fig. 8. This dynamic method is an online real-time approach, so measurements must be obtained continuously for early fault detections.

## V. NUMERICAL RESULTS

The implementation of the online condition monitoring approach for the battery systems are performed with MATLAB/Simulink programs by using the experimental current measurements of the Ni-MH battery system. The nonlinear estimator gain is selected as  $\delta_1 = 2$  (note that since the nonlinear estimator is robust, this gain should not be selected very large in order to have high sensitivity to faults). Initial conditions for estimator are taken as  $T_o = 19^\circ\text{C}$  and  $V_{co} = 0$ . For threshold calculations, the mean and standard deviation of voltage and temperature residuals, by considering their root mean square (rms) values, are found as  $\mu_V = 0.44$ ,  $\sigma_V = 0.65$ ,  $\mu_T = 0.0004$ , and  $\sigma_T = 0.0004$ . The rms functions of the residuals are used in the residual evaluations. For the estimator, the  $\text{sat}(\cdot)$  function defined below is used instead of the  $\text{sign}(\cdot)$  function in order to ease numerical calculations via continuous approximation.

$$\text{sat}(e) = \begin{cases} e/|e|, & |e| > 1 \\ e, & |e| \leq 1. \end{cases} \quad (14)$$

Fig. 9 displays the load current and the SOC estimation for an initial value 60% and under normal operating conditions. While the SOC is a difficult parameter to predict in the battery management system, the current integral method is commonly used to estimate SOC and provides information about remaining useful energy and the remaining usable time of the battery.

Different faults on measurements and battery parameters are considered for fault diagnosis as given in Table II. Several incipient type faults are injected into the battery system for diagnosis since the detection of incipient faults is most difficult. Fig. 10 illustrates a voltage sensor fault and its detection using the voltage residual  $r_V$ . It is obvious from the figure that once an incipient voltage sensor fault occurs, it is detected and isolated via residual surpassing the threshold  $R_V$ .

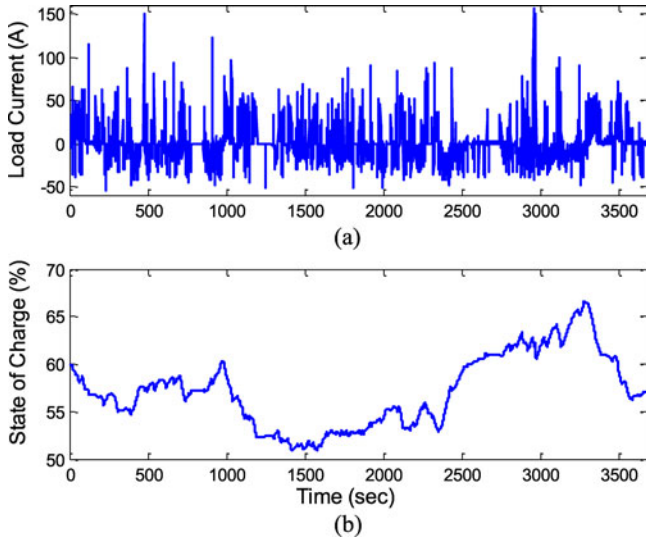


Fig. 9. SOC estimation from the load current. (a) Load current. (b) SOC estimation.

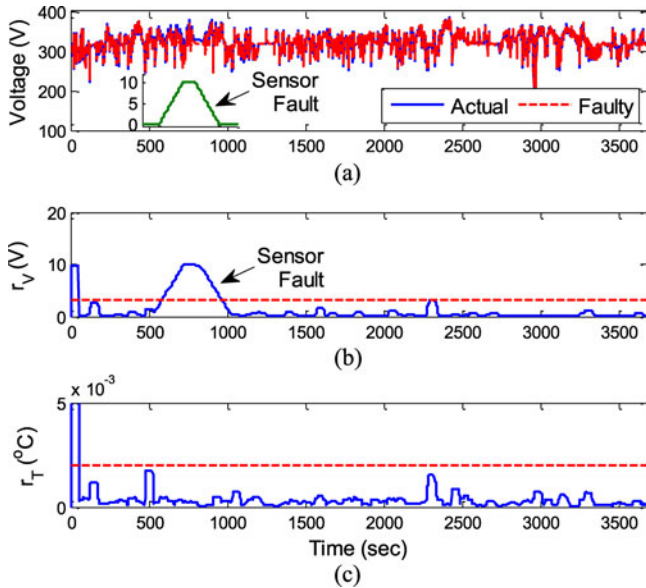


Fig. 10. Voltage sensor fault and its monitoring. (a) Time response of voltage. (b) Residual  $r_v$ . (c) Residual  $r_T$ .

In Fig. 11, it is assumed that the temperature controller failed at the time  $t = 3000$  s. This failure is detected by temperature residual  $r_T$ . The figure shows that the controller failure immediately affects the temperature residual so that the residual exceeds the threshold  $R_T$ .

An incipient temperature sensor fault that is injected into the battery system is depicted in Fig. 12. The temperature and voltage residuals immediately exceed their threshold values to indicate the existence of temperature sensor fault. We can observe from figures that the nonlinear estimator exhibits robustness characteristics, which is important for healthy online condition monitoring. It should be noted that  $r_V$  may not exceed its threshold for small temperature sensor fault values unless the threshold is decreased, but then there will be some false alarms.

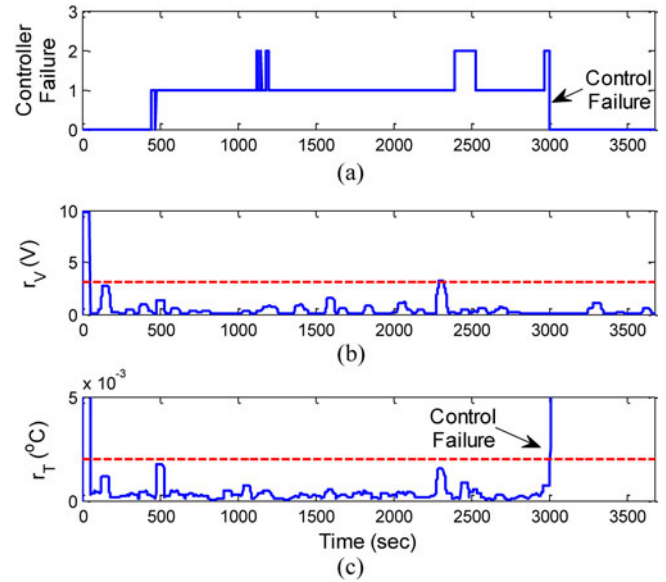


Fig. 11. Control (fan) failure and its detection. (a) Control signal [unitless, see (5)]. (b) Residual  $r_v$ . (c) Residual  $r_T$ .

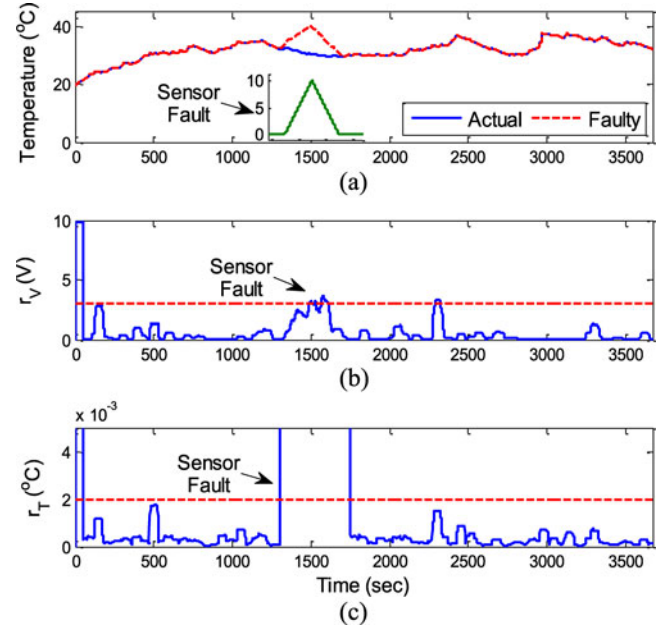


Fig. 12. Temperature sensor fault and its detection. (a) Time response of temperature. (b) Residual  $r_v$ . (c) Residual  $r_T$ .

An unexpected deviation in the internal resistance of the battery is shown in Fig. 13. A small and drift-like deviation in the resistance results in alarms in voltage and temperature residuals by exceeding thresholds. The internal resistance of battery provides knowledge about several problems, including grid growth, sulfation, dry out, and corrosion. Hence, the diagnosis of internal resistance fault is an important aspect of the methodology in terms of its good performance and efficiency.

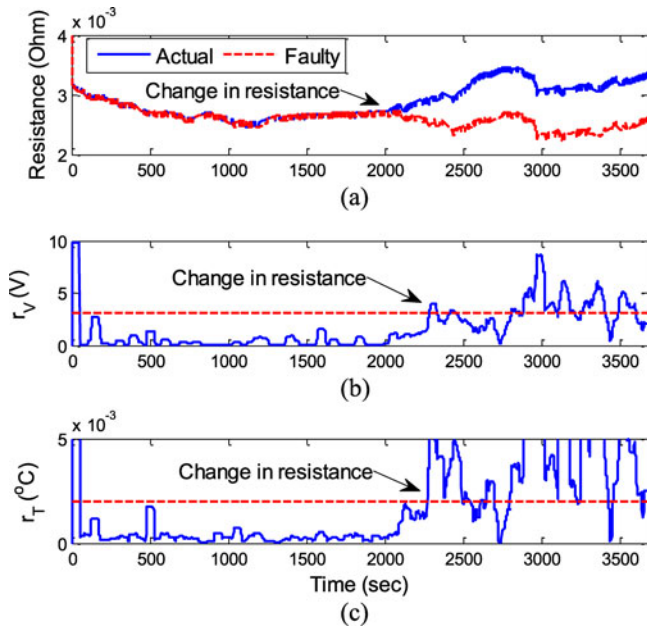


Fig. 13. Internal resistance deviation and its detection. (a) Time response of internal resistance. (b) Residual  $r_v$ . (c) Residual  $r_T$ .

## VI. CONCLUSION

This paper proposed a nonlinear estimator-based online condition monitoring system for battery systems used in the industry. The study set out to determine the possibility of online battery health monitoring system based on battery modeling and detection of internal battery problems. This research has shown that the nonlinear estimator-based approach provides a robust and efficient fault diagnosis for internal faults through detection of internal cell resistance deviations, measurement faults, and temperature controller failure in the battery system. The results of this study indicate that the proposed online real-time health monitoring approach can provide early fault detection, extended useful life, better maintenance, and optimized replacement timing for battery systems.

## ACKNOWLEDGMENT

The author gratefully would like to thank Prof. G. Rizzoni, the Director of the Center for Automotive Research, Ohio State University, for his valuable guidance and contributions.

## REFERENCES

- [1] M. A. Fetcenko, S. R. Ovshinsky, B. Reichman, K. Young, C. Fierro, J. Koch, A. Zallen, W. Mays, and T. Ouchi, "Recent advances in NiMH battery technology," *J. Power Sources*, vol. 165, pp. 544–551, 2007.
- [2] D. Kim and H. Cha, "Analysis on lead-acid battery bank for nuclear power plants in Korea," in *Proc. Int. Power Electron. Motion Control Conf.*, 2012, vol. 3, pp. 2118–2122.
- [3] N. K. Trehan, "Impact of failures of direct current systems on nuclear power generating stations," in *Proc. IEEE Nucl. Sci. Symp. Conf. Rec.*, 2001, vol. 4, pp. 2482–2485.
- [4] S. Eckrood and B. M. Radimer, "Review of engineering design considerations for battery energy management systems," *IEEE Trans. Energy Convers.*, vol. 6, no. 2, pp. 303–309, Jun. 1991.
- [5] P. M. Frank and X. Ding, "Survey of robust residual generation and evaluation methods in observer-based fault detection systems," *J. Process Control*, vol. 7, no. 6, pp. 403–424, 1997.
- [6] R. Isermann, "Model-based fault-detection and diagnosis—Status and applications," *Annu. Rev. Control*, vol. 29, no. 1, pp. 71–85, 2005.
- [7] R. Isermann, *Fault-Diagnosis Systems*. New York, NY, USA: Springer-Verlag, 2006.
- [8] J. Gertler, *Fault Detection and Diagnosis in Engineering Systems*. New York, NY, USA: Marcel Dekker, 1998.
- [9] C. Hajjiye and F. Caliskan, *Fault Diagnosis and Reconfiguration in Flight Control Systems*. Norwell, MA, USA: Kluwer, 2003.
- [10] J. Zhang and J. Lee, "A review on prognostics and health monitoring of Li-ion battery," *J. Power Sources*, vol. 196, pp. 6007–6014, 2011.
- [11] X. Tang, X. Zhang, B. Koch, and D. Frisch, "Modeling and estimation of nickel metal hydride battery hysteresis for SOC estimation," presented at the Int. Conf. Prognostics Health Manage., Denver, CO, USA, 2008.
- [12] C. Suozzo, S. Onori, and G. Rizzoni, "Model-based fault diagnosis for NiMH battery," presented at the 1st Annu. Dyn. Syst. Control Conf., Ann Arbor, MI, USA, 2009.
- [13] M. V. Micea, L. Ungurean, G. N. Cârstoiu, and V. Groza, "Online State-of-health assessment for battery management systems," *IEEE Trans. Instrum. Meas.*, vol. 60, no. 6, pp. 1997–2006, Jun. 2011.
- [14] D. Ilic, M. Kilb, K. Holl, H. Praas, and E. Pytlík, "Recent progress in rechargeable nickel/metal hydride and lithium-ion miniature rechargeable batteries," *J. Power Sources*, vol. 80, no. 1–2, pp. 112–115, 1999.
- [15] D. Linden and T. B. Reddy, *Handbook of Batteries*, 3rd ed. New York, NY, USA: McGraw-Hill, 2001.
- [16] Y. Kim and H. Ha, "Design of interface circuits with electrical battery models," *IEEE Trans. Ind. Electron.*, vol. 44, no. 1, pp. 81–86, Feb. 1997.
- [17] A. C. Margaret and M. Salameh, "Determination of lead-acid battery via mathematical model techniques," *IEEE Trans. Energy Convers.*, vol. 7, no. 3, pp. 442–446, Sep. 1992.
- [18] J. Zhang, S. Ci, H. Sharif, and M. Alahmad, "Modeling discharge behavior of multicell battery," *IEEE Trans. Energy Convers.*, vol. 25, no. 4, pp. 1133–1141, Dec. 2010.
- [19] T. Kim and W. Qiao, "A hybrid battery model capable of capturing dynamic circuit characteristics and nonlinear capacity effects," *IEEE Trans. Energy Convers.*, vol. 26, no. 4, pp. 1172–1180, Dec. 2011.
- [20] B. Paxton and J. Newmann, "Modeling of nickel/metal hydride batteries," *J. Electrochem. Soc.*, vol. 144, no. 11, pp. 3818–3831, 1997.
- [21] W. B. Gu and C. Y. Wang, "Thermal-electrochemical modeling of battery systems," *J. Electrochem. Soc.*, vol. 147, no. 8, pp. 2910–2922, 2000.
- [22] V. Srinivasan and C. Y. Wang, "Analysis of electrochemical and thermal behavior of Li-ion cells," *J. Electrochem. Soc.*, vol. 150, no. 1, pp. A98–A106, 2003.
- [23] V. Agarwal, K. Uthaichana, R. A. DeCarlo, and L. H. Tsoukalas, "Development and validation of a battery model useful for discharging and charging power control and lifetime estimation," *IEEE Trans. Energy Convers.*, vol. 25, no. 3, pp. 821–835, Sep. 2010.
- [24] C. Zhou, K. Qian, M. Allan, and W. Zhou, "Modeling of the cost of EV battery wear due to V2G application in power systems," *IEEE Trans. Energy Convers.*, vol. 26, no. 4, pp. 1041–1050, Dec. 2011.
- [25] O. Tremblay and L. A. Dessaint, "Experimental validation of a battery dynamic model for EV applications," *World Electr. Veh. J.*, vol. 3, pp. 1–10, 2009.
- [26] C. R. Gould, C. M. Bingham, D. A. Stone, and P. Bentley, "New battery model and state-of-health determination through subspace parameter estimation and state-observer techniques," *IEEE Trans. Veh. Technol.*, vol. 58, no. 8, pp. 3905–3916, Oct. 2009.
- [27] J. Marcos, A. Lago, C. M. Penalver, J. Doval, A. Nogueira, C. Castro, and J. Chamadoira, "An approach to real behaviour modeling for traction lead-acid batteries," in *Proc. IEEE 32nd Annu. Power Electron. Spec. Conf.*, 2001, vol. 2, pp. 620–624.
- [28] A. Emadi, M. Ehsani, and J. M. Miller, *Vehicular Electric Power Systems*. New York, NY, USA: Marcel Dekker, 2004.
- [29] V. H. Johnson, "Battery performance models in ADVISOR," *J. Power Sources*, vol. 110, no. 2, pp. 321–329, Aug. 2002.
- [30] H. He, R. Xiong, and J. Fan, "Evaluation of lithium-ion battery equivalent circuit models for state of charge estimation by an experimental approach," *Energies*, vol. 4, no. 12, pp. 582–598, 2011.
- [31] S. Piller, M. Perrin, and A. Jossen, "Methods for state-of-charge determination and their applications," *J. Power Sources*, vol. 96, no. 1, pp. 113–120, Jun. 2001.
- [32] S. Lee, J. Kim, J. Lee, and B. H. Cho, "The state and parameter estimation of an Li-ion battery using a new OCV-SOC concept," presented at the IEEE Power Electron. Spec. Conf., Orlando, FL, USA, 2007.
- [33] L. Liu, L. Y. Wang, Z. Chen, C. Wang, F. Lin, and H. Wang, "Integrated system identification and state-of-charge estimation of battery systems," *IEEE Trans. Energy Convers.*, vol. 28, no. 1, pp. 12–23, Mar. 2013.

- [34] S. R. Logan, "The origin and status of the Arrhenius equation," *J. Chem. Educ.*, vol. 59, no. 4, p. 279, Apr. 1982.
- [35] G. Ablay and T. Aldemir, "Observation of the dynamics of nuclear systems using sliding mode observers," *Nucl. Technol.*, vol. 174, no. 1, pp. 64–76, 2011.
- [36] G. Ablay and T. Aldemir, "Fault detection in nuclear systems using sliding mode observers," *Nucl. Sci. Eng.*, vol. 173, no. 1, pp. 82–98, 2013.
- [37] M. Basseville and I. V. Nikiforov, *Detection of Abrupt Changes: Theory and Application*. Englewood Cliffs, NJ, USA: Prentice-Hall, 1993.

Author's photograph and biography not available at the time of publication.